



Temperature and depth distribution of Japanese eel eggs estimated using otolith oxygen stable isotopes

Kotaro Shirai^{a,*}, Tsuguo Otake^{b,*}, Yosuke Amano^c, Mari Kuroki^b,
Takayuki Ushikubo^{d,e}, Noriko T. Kita^e, Masafumi Murayama^f,
Katsumi Tsukamoto^g, John W. Valley^e

^a Atmosphere and Ocean Research Institute, The University of Tokyo, 5-1-5 Kashiwanoha, Kashiwa, Chiba 277-8564, Japan

^b Graduate School of Agricultural and Life Sciences, The University of Tokyo, 1-1-1 Yayoi, Bunkyo, Tokyo 113-8657, Japan

^c Tohoku National Fisheries Research Institute, Fisheries Research Agency, Shiogama, Miyagi 985-0001, Japan

^d Kochi Institute for Core Sample Research, Japan Agency for Marine-Earth Science and Technology (JAMSTEC), Monobe B200, Nankoku, Kochi 783-8502, Japan

^e WiscSIMS, Department of Geoscience, University of Wisconsin, Madison, WI 53706, USA

^f Center for Advanced Marine Core Research, Kochi University, B200 Monobe, Nankoku, Kochi 783-8502, Japan

^g College of Bioresource Sciences, Nihon University, 1866 Kameino, Fujisawa, Kanagawa 252-0880, Japan

Received 24 April 2017; accepted in revised form 3 March 2018; available online 12 March 2018

Abstract

Oxygen isotope ratios of the core region of otoliths were examined in *Anguilla japonica* glass eels collected from two rivers in Japan to verify the possible temperature and depth layer experienced by these eels when they were at the egg stage in their spawning area. To determine the relationship between otolith $\delta^{18}\text{O}$ values and water temperature, the otoliths of glass eels reared under four different temperatures (15, 20, 25 and 30 °C) were analyzed. The otolith $\delta^{18}\text{O}$ values showed an inverse relationship to ambient water temperature. Linear regression of the fractionation between otolith oxygen isotopic ratio from the $\delta^{18}\text{O}$ of seawater and water temperature produced a precisely determined relationship from 15 to 30 °C: $\delta^{18}\text{O}_{\text{otolith,PDB}} - \delta^{18}\text{O}_{\text{seawater,SMOW}} = -0.153 \times T (\text{°C}) + 1.418$. The $\delta^{18}\text{O}_{\text{core,PDB}}$ values of the otolith core region of the glass eels from the two locations were -2.53 ± 0.12 and -2.59 ± 0.07 respectively, and could be converted to water temperatures of 26.3 ± 0.8 °C and 26.7 ± 0.4 °C, respectively, using the equation and assuming a seawater $\delta^{18}\text{O}_{\text{seawater,SMOW}} = 0.06\text{‰}$. The water depth corresponding to these temperatures is ~ 150 m in the water column in the spawning area of Japanese eels, which corresponds to the upper-most part of the thermocline and chlorophyll maximum in the vertical hydrographic profile. These results were consistent with the field studies that egg development after the beginning of otolith formation and hatching occurs around the upper-most part of thermocline, suggesting that stable isotope micro-analysis is a powerful method to extrapolate unknown spawning ecology of fishes.

© 2018 Elsevier Ltd. All rights reserved.

Keywords: *Anguilla japonica*; Glass eel; Oxygen stable isotopes; SIMS; Otolith; Spawning temperature and depth

1. INTRODUCTION

The unusual life history of anguillid eels has fascinated scientists for more than a century, and efforts to learn about their ecology have increased in recent years due to declines

* Corresponding authors.

E-mail addresses: kshirai@aori.u-tokyo.ac.jp (K. Shirai), otake@aqua.fs.a.u-tokyo.ac.jp (T. Otake).

in their population. The European eel *Anguilla anguilla* was registered as an endangered species in 2006 and remarkable population declines have been observed in two other species of temperate freshwater eels, the American eel *A. rostrata* and Japanese eel *A. japonica* during recent decades (Casselman, 2003; Dekker, 2003; Tsukamoto et al., 2009a; ICES, 2010; Kuroki et al., 2014). The Japanese eel has recently been registered as a Level II endangered species by the Ministry of Environment of Japan in 2013 (http://www.env.go.jp/press/file_view.php?serial=21437&hou_id=16264), as well as registered as IUCN Red List of Threatened Species (Jacoby et al., 2015). It has remained difficult to clearly determine the reasons for the declines in anguillid eels that may include many factors ranging from habitat loss and overfishing, and toxins and parasites, to changes in the ocean-atmosphere system (Feunteun, 2002; Knights, 2003; Friedland et al., 2007; Miller et al., 2009) in part because so little is known about their spawning ecology (Lecomte-Finiger, 1994).

Efforts to reduce fishing pressure on anguillid glass eels such as the Japanese eel have been centered on developing artificial production of glass eels for seed in aquaculture. These efforts depend on a clear understanding of the spawning biology and early life history of the leptocephalus larvae of eels, which has remained very limited. Recent captures of mature adult eels (Chow et al., 2009; Kurogi et al., 2011; Tsukamoto et al., 2011), preleptocephali just after hatching (early development stage eel larvae) (Tsukamoto, 2006; Tsukamoto et al., 2011), the fertilized eggs of Japanese eel (Tsukamoto et al., 2011) near the West Mariana Ridge, and compilation of collection data with oceanohydrographic structures (Aoyama et al., 2014; Schabetsberger et al., 2016) have provided new information about the mysterious spawning ecology of eels. However, details about the actual temperature and depth of spawning and hatching, which are vital for improved understanding of the spawning ecology and physiology and early life history of the progeny, are still vague. Artificial spawning and rearing of the Japanese eel in Japan has succeeded to complete their life cycle in captivity by spawning adult females that were reared throughout their life from hatching to spawning in the laboratory (Tanaka, 2011). There still remain many problems including low survival and deformities of larvae in the process of artificial production (Okamura et al., 2007; Kurokawa et al., 2008; Okamoto et al., 2009; Kuroki et al., 2016), so more information about the natural life history of the Japanese eel should be examined from various aspects.

The oxygen stable isotope ratios ($\delta^{18}\text{O}$) in otolith aragonite have been shown to be at or near isotopic equilibrium with the ambient water for several fish species, with fractionation being controlled by temperature (Kalish, 1991a, b; Radtke et al., 1996; Thorrold et al., 1997; Campana, 1999; Høie et al., 2004; Walther and Thorrold, 2009; Hanson et al., 2010; Kitagawa et al., 2013). Otolith $\delta^{18}\text{O}$ values have been used to help understand the migration behavior and thermal requirements in commercially and ecologically important species such as haddock (Begg and Weidman, 2001), Atlantic cod (Gao et al., 2001b), orange roughy (Shephard et al., 2007), Pacific halibut (Gao and

Beamish, 2003), sockeye salmon (Gao and Beamish, 1999), common sole (Morat et al., 2014) and Pacific herring (Gao et al., 2001a). Conventional mass spectrometry for otolith stable isotope analysis requires extraction of a certain amount of otolith sample (i.e. >several μg of otolith powder), which limits a temporal resolution of reconstruction, especially being problematic when focusing on otoliths core and the periphery. Recent development of Secondary Ion Mass Spectrometry (SIMS) allowed the analysis of stable isotope composition with a remarkably fine lateral spatial resolution at a scale of only several micrometers with reasonable precision (Weber et al., 2005; Weidel et al., 2007; Sano et al., 2008; Kozdon et al., 2009; Valley and Kita, 2009; Hanson et al., 2010; Matta et al., 2013; Limburg et al., 2013; Hogan et al., 2017). The microanalysis of otolith $\delta^{18}\text{O}$ can provide reliable information about the temperature environment experienced by individual fish with time resolution corresponding to particular daily ages and life history stages.

In the present study, we demonstrate a method to estimate the hatching temperature and depth of Japanese eel experimentally in the laboratory. We examined $\delta^{18}\text{O}$ of otolith core in glass eels (Japanese eel) to determine the possible temperature and depth layer in the ocean of these individuals when they were at the egg stage. Since the core region of eel otoliths is quite tiny, only 10–20 μm diameter, high spatial resolution SIMS is the only method that allows analysis of this domain. We performed SIMS analysis for the otolith core region using an 8 μm diameter spot inside of the hatch check (core region), which completely avoids contamination by isotopic signals from outside of the core. To apply otolith $\delta^{18}\text{O}$ values as a thermometer, we first assessed the relationship between water temperature and otolith $\delta^{18}\text{O}$ values of glass eels reared under four different temperatures (15, 20, 25 and 30 °C). The estimated depth layer where each glass eel may have been distributed during its egg stage was then determined by comparing the water temperature estimated from $\delta^{18}\text{O}$ values of the otolith core region to the temperature corresponding to a specific depth within an actual vertical profile of water temperature in the spawning area of the Japanese eel near the West Mariana Ridge.

2. MATERIALS AND METHODS

2.1. Fish used for otolith analyses

Freshwater eels are catadromous fish species that breed at sea and grow in freshwater. They hatch in shallow waters of deep ocean and the larvae, so called leptocephali, are transported in currents and recruit to rivers after metamorphosis into juvenile glass eels. Otoliths formation occurs during embryonic stage, and a laboratory experiment on artificially fertilized eggs showed that the primordium (the initial complex structure of an otolith core) of the otoliths of Japanese eels start to be formed at 13–15 h and 30–35 h after fertilization during 23–28 h and 48–54 h incubation periods until hatching, at 28 °C and 19 °C, respectively (Ahn et al., 2012). Thus, the $\delta^{18}\text{O}$ values of the otolith core region reflect the ambient water temperature in the later 1/3

to 1/2 of the total egg development period. The oxygen isotope analysis of the otolith core regions was carried out using two different groups of glass eels collected in Japan. One group of 26 glass eels was collected from the Tone River of north-central Japan using a hand net on February 1998 and preserved in 99.5% ethanol. The other group, totaling 120 glass eels, was collected from the Hamana Lake (9.8 °C, salinity 33.9 psu) in central Japan on February 2006 using a commercial fishing set net. These eels collected in Hamana Lake were used for the rearing

experiment to determine the relationship between otolith oxygen isotope ratios ($\delta^{18}\text{O}$) and ambient water temperature (Table 1).

The glass eels collected from Hamana Lake were kept in a polystyrene box with natural seawater and brought to the IRAGO Institute, Aichi Prefecture, Japan, where the rearing experiment was conducted. The glass eels were then kept in four tanks (10 l, 295 mm × 445 mm × 253 mm; polypropylene ABS resin) containing natural seawater (salinity 32.0 psu). Each tank was equipped with an air-

Table 1

Characteristics of the glass eels used in experiments for each temperature treatment group in the present study (from Fukuda et al. 2009).

Water temperature (°C)	Number of fish	Total length (mm) (mean ± SD)	Body weight (g) (mean ± SD)	Survival rate (%)
15	3	61.1 ± 3.1	0.18 ± 0.03	100
20	7	60.8 ± 1.8	0.22 ± 0.02	100
25	7	65.1 ± 3.5	0.20 ± 0.03	100
30	4	60.4 ± 3.8	0.15 ± 0.04	74

Total length and body weight present those at the end of 30 days rearing period.

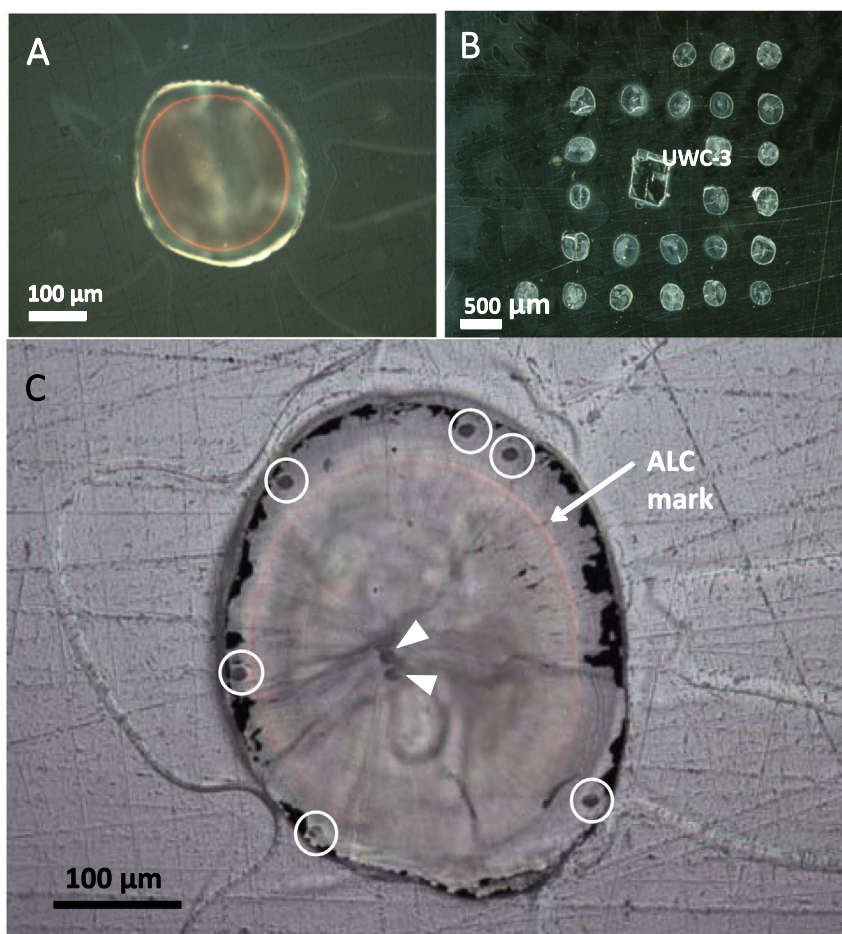


Fig. 1. (A) An otolith of Japanese eel used in the present experimental study that was marked with alizarin complexone (ALC) with the orange ALC mark showing the timing of the beginning of the temperature treatments. (B) A sample set including 25 otoliths (Sample-A) from glass eels reared in four tanks at different temperatures (15, 20, 25 and 30 °C) and a piece of an analysis standard (calcite: UWC-3). (C) An otolith analyzed by SIMS showing six analysis spots outside of the ALC mark (circles) that were used for determination of the relationship between otolith $\delta^{18}\text{O}$ and water temperature, and two analysis spots within the otolith core region (arrowheads) that were used for estimation of the temperature and depth layer experienced during the egg stage.

stone to aerate the water and two 80 mm polyvinyl chloride (PVC) pipes in which glass eels could shelter and were set in a water bath with temperature controlled at 15 °C. The otoliths of each glass eel were then marked by adding alizarin complexone (ALC, 10–15 °C to a concentration of 100 ppm) for 16 h (Fig. 1A). After otolith staining with ALC to mark the timing of the beginning of the temperature treatments, they were transferred to four different experimental tanks of the same size with seawater (salinity 32.0 psu). Thirty glass eels were put in each experimental tank, which were set in separate water baths and maintained at water temperatures of 15, 20, 25 or 30 °C, during the rearing period of 30 days. The water temperature of each water bath was gradually changed to the respective temperatures from the initial temperature of 15 °C over 24 h after the glass eels were transferred. Glass eels were reared under a 12L:12D photoperiod and were fed an excess of *Chironomus* sp. larvae (Kyorin Co. Ltd., Japan) each day. A portion of the rearing water (2 L, 20% of water) in each tank was exchanged every day with fresh seawater at each respective temperature. The survival rate of glass eels was 74% in the 30 °C treatment, but survival was 100% in the other temperatures. Details are reported in Fukuda et al. (2009). The glass eels were frozen at –20 °C after the rearing experiment finished, and their body lengths were measured and developmental stages determined before the extraction of their otoliths.

2.2. Otolith preparation for SIMS analysis

Sagittal otoliths were extracted from each glass eel. After washing with ion-free water, two otolith sample sets were embedded in epoxy resin together with the UWC-3 calcite standard (Kozdon et al., 2009) produced by the University of Wisconsin for SIMS oxygen isotope analysis (Fig. 1B). One sample set (Sample-A) was composed of 25 otoliths from the Hamana Lake fish reared in four tanks of different temperatures (7, 7, 7 and 4 otoliths from fish of 15, 20, 25 and 30 °C, respectively) (Fig. 1B). Otoliths used for the Sample-A were randomly selected from each tank. The other set (Sample-B) included 26 otoliths of glass eels from the Tone River. An otolith from left or right was randomly chosen.

Each otolith was ground to expose the core region using a grinding machine equipped with 56 µm and 13 µm diamond cup-whetstones (Diskoplan TS, Marumoto Strues,

Co. Ltd. Japan). They were then polished with 1–6 µm diamond films to make a completely flat low-relief surface for SIMS analysis. Otoliths and standards were coated with gold after polishing and cleaning. Twenty-one of 25 otoliths (3 from 15 °C, 7 from 20 °C, 7 from 25 °C, 4 from 30 °C) in Sample-A were successfully ground and polished. The otolith edge portion outside of the ALC mark in each otolith of Sample-A, which was formed during the 30-day rearing experiment, was used for assessing the relationship between otolith $\delta^{18}\text{O}$ values and ambient water temperature (Table 2, Fig. 1C). Four of the 21 otoliths in Sample-A and four of the 26 otoliths in Sample-B that had a wider area of their core region successfully exposed, were further used for the otolith $\delta^{18}\text{O}$ thermometry study to determine the water temperature experienced by the glass eels during their egg stage. The core regions of the other otoliths were not the same level and was not exposed to the surface and thus could not be analyzed. No significant difference in otolith textures were observed between Sample-A and Sample-B in cross section, likely indicating that there is effect due to storage in ethanol. A total of 74 analyses in 21 otoliths in Sample-A were also used for the comparison of the otolith $\delta^{18}\text{O}$ values to otolith growth patterns.

2.3. Ion microprobe oxygen isotope analyses of otoliths

Oxygen isotope analyses were performed at the WiscSIMS Laboratory, University of Wisconsin, using a CAMECA ims-1280 high resolution, multi-collector ion microprobe and analytical protocols described previously (Weidel et al., 2007; Kita et al., 2009; Kozdon et al., 2009). We used a $^{133}\text{Cs}^+$ primary ion beam with an intensity of 1.7–1.8 nA, which was focused to a spot size of approximately 8 µm diameter. The secondary O^- ions were detected simultaneously by two Faraday cups. The typical count rate of $^{16}\text{O}^-$ was $3.2\text{--}3.5 \times 10^9$ cps. Total analytical time per spot was about 3 min including pre-sputtering (10 s), automatic centering of the secondary ions (~80 s), and analysis (80 s). Four to six spots were analyzed in the outer margin of each otolith along with one or two spots within the core region, which were carefully positioned (Fig. 1C).

Small pieces of UWC-3 calcite standard that were mounted in the center of each sample (Fig. 1B) were measured in at least four spots before and after every <13 spot analyses, and the resulting average value bracketing the

Table 2

$\delta^{18}\text{O}$ values of rearing seawater, number of otolith analyzed, otolith growth at analysis point during 30 days rearing period, $\delta^{18}\text{O}$ values of otolith portion precipitated during the rearing period and fractionation of otoliths $\delta^{18}\text{O}$ the ratio of rearing seawater.

Water temperature (°C)	$\delta^{18}\text{O}_{\text{seawater}}$ (‰, SMOW)	Number of otolith	Number of analysis points	Otolith growth (µm/30 days)	Otolith $\delta^{18}\text{O}$ (‰, PDB) (mean ± SD)	Otolith $\delta^{18}\text{O}$ minus $\delta^{18}\text{O}$ of rearing seawater (‰, PDB) (mean ± SD)
15	-0.26 ± 0.12	3	10	17.1 ± 3.67	-1.01 ± 0.03	-0.75 ± 0.12
20	-0.15 ± 0.10	7	25	34.2 ± 9.16	-1.81 ± 0.19	-1.66 ± 0.21
25	0.05 ± 0.08	7	22	39.8 ± 11.1	-2.43 ± 0.14	-2.48 ± 0.16
30	-0.05 ± 0.29	4	17	39.2 ± 13.4	-3.08 ± 0.15	-3.03 ± 0.33

Otolith $\delta^{18}\text{O}$ value is presented as a mean of representative ratio for each otolith that is the average of 3–7 points in each otolith.

samples was used for instrumental drift correction. The instrumental bias and the matrix effect are stable and almost constant within the analytical uncertainty as far as we keep the same analytical condition within a single session (see Fig. 3 in Kita et al., 2009). For this reason, we frequently measured standard analyses to confirm the stability of the analytical condition in every session. All $\delta^{18}\text{O}$ values (in permil, ‰) of otolith rims or cores are presented relative to the Vienna Pee Dee Belemnite (VPDB) scale ($\delta^{18}\text{O}_{\text{otolith, PDB}}$ or $\delta^{18}\text{O}_{\text{core, PDB}}$, respectively). For oxygen isotope ratios of biogenic calcium carbonate, comparison of $\delta^{18}\text{O}_{\text{carbonate, PDB}}$ and $\delta^{18}\text{O}_{\text{water SMOW}}$ is commonly used (see Wanamaker et al., 2007; Paleoceanography, for example). We added two scales of the Y-axis when needed, one for alpha and another for $\delta^{18}\text{O}_{\text{carbonate, PDB}}$ and $\delta^{18}\text{O}_{\text{water SMOW}}$. Reproducibility of the individual spot analyses of UWC-3 standard (bracketing analyses; $n \sim 8$) was assigned as the precision of a single analysis, which is typically 0.3–0.4‰ (2 SD). The variability within each otolith is presented as the standard deviation of all spots in each individual otolith (2 SD).

These procedures have been shown to produce accurate and precise values for oxygen isotope ratio in abiogenic calcite (Kita et al., 2009; Valley and Kita, 2009), but analysis of biogenic aragonite introduces the possibility of a systematic offset in $\delta^{18}\text{O}$. The SIMS technique is comparative and there is no theoretical basis for comparing samples that differ from calibration standards in mineralogy or chemical composition. At the time of analysis, there were no reliable standards for aragonite or for biogenic carbonates that contain even trace amounts of water or organic matter. Recently, estimates of these effects suggest that there could be a systematic difference in matrix effect (instrument bias) of up to 2‰ for biogenic aragonite causing low $\delta^{18}\text{O}$ values (Orland et al., 2015; Linzmeier et al., 2016; Sliwinski et al., 2017), which has not been clarified when this work was performed in 2008. Importantly, this study compares SIMS analyses of natural vs. lab-reared otoliths. The UWC-3 calcite is used as a running standard and thus any systematic offset in $\delta^{18}\text{O}$ (otolith) due to matrix effects will have no effect on relative differences between otoliths or on the oxygen isotope temperatures that are calibrated by the same standard. Thus the conclusions of this study are not affected by choice of standard.

2.4. Oxygen isotope analysis of rearing water

To determine the isotopic fractionation factor for O between the otolith and the ambient water with different temperatures, we examined the $\delta^{18}\text{O}$ of the rearing water of each tank collected at the beginning, middle and the end of the rearing experiment (0, 15, 30 days after the start of rearing). Fifty ml of rearing water was sampled for mass spectrometry.

The oxygen isotope ratio of the water was determined using the conventional headspace $\text{CO}_2\text{-H}_2\text{O}$ equilibration technique (e.g. Epstein and Mayeda, 1953). Equilibrated CO_2 in the headspace was analyzed with a dual-inlet stable isotope mass spectrometer IsoPrime, installed at the Kochi Core Center of JAMSTEC in Japan. The analytical precision

of the measurements was 0.1‰ for $\delta^{18}\text{O}$ values based on the reproducibility of laboratory standards. All $\delta^{18}\text{O}$ values of water are presented in Table 2 as the Vienna Standard Mean Ocean Water (V-SMOW) scale ($\delta^{18}\text{O}_{\text{seawater, V-SMOW}}$). For calculating a fractionation factor between seawater and otolith, $R_{\text{PDB}}/R_{\text{VSMOW}}$ value of 1.03091 (Coplen et al., 1983) was used.

2.5. Otolith growth effects on $\delta^{18}\text{O}$ values

Growth-rate-related kinetic disequilibrium in skeletal $\delta^{18}\text{O}$ has been widely observed in corals (e.g. McConnaughey, 1989). However, there is only limited information about possible growth effects on $\delta^{18}\text{O}$ of otoliths (e.g. Geffen, 2012). Some intra- and inter-otolith growth variations during the 30-day rearing period within the same temperature treatment were evident and seen as variable distance from ALC marks to otolith edge (Fig. 1A, C). To examine the effect of otolith growth rate on the fractionation of otolith $\delta^{18}\text{O}$ values, the $\delta^{18}\text{O}$ values were compared among otolith portions with different widths outside the ALC mark. To do this, we used a total of 74 $\delta^{18}\text{O}$ values from analysis points in 21 otoliths in Sample-A, which were located on the otolith margin outside of the ALC mark in areas with various growth patterns. Each otolith space outside the ALC mark was measured under an optical microscope fitted with an image processor. The relationships between the otolith growth rates and $\delta^{18}\text{O}$ values were examined for the four different water temperature treatments.

3. RESULTS

The mean $\delta^{18}\text{O}$ values of the otolith edge precipitated during the 30-day rearing period under 15, 20, 25 and 30 °C were -1.01 ± 0.03 (1 SD, $n = 3$), -1.81 ± 0.19 ($n = 7$), -2.43 ± 0.14 ($n = 7$), and -3.08 ± 0.15 ‰ ($n = 4$), respectively. There was a significant difference among the $\delta^{18}\text{O}$ values of four temperatures (Table 2, *F*-test, ANOVA, $p < 0.01$) with an inverse relationship to ambient water temperature (Fig. 2) presented as following equation:

$$\delta^{18}\text{O}_{\text{otolith, PDB}} = -0.130 \times T(^{\circ}\text{C}) + 0.822 \quad (r^2 = 0.89) \quad (1)$$

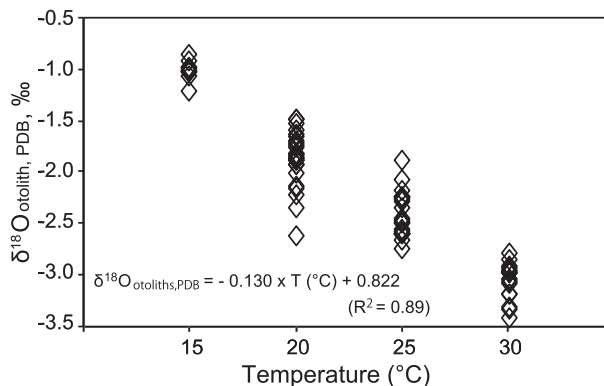


Fig. 2. The relationship between otolith $\delta^{18}\text{O}$ and rearing water temperature on Japanese eel. Each data point shows individual spot of the analysis.

The mean $\delta^{18}\text{O}$ values (1 SD) of seawater used for the rearing at temperatures of 15, 20, 25 and 30 °C were -0.26 ± 0.12 , -0.15 ± 0.10 , -0.05 ± 0.08 , and $-0.05 \pm 0.29\text{‰}$, respectively (Table 2). The otolith $\delta^{18}\text{O}$ fractionation relative to the rearing seawater is described as following; $\delta^{18}\text{O}_{\text{Otolith,PDB}} - \delta^{18}\text{O}_{\text{seawater,SMOW}}$, at temperatures of 15, 20, 25 and 30 °C were -0.75 ± 0.12 (mean \pm SD), -1.66 ± 0.21 , -2.48 ± 0.16 and $-3.03 \pm 0.33\text{‰}$, respectively (Table 2, Fig. 3). When described using the fractionation factor, $1000 \ln \alpha$ (otolith – seawater) at 15, 20, 25 and 30 °C, the values are 29.65 ± 0.12 (mean \pm SD), 28.75 ± 0.21 , 27.91 ± 0.16 , and 27.37 ± 0.33 , respectively.

There remained a significant difference among the four $\delta^{18}\text{O}$ values (F -test, ANOVA, $p < 0.01$) and a strong inverse relationship between $\delta^{18}\text{O}_{\text{Otolith}} - \delta^{18}\text{O}_{\text{seawater}}$ and temperature ($-0.153\text{‰ } ^\circ\text{C}^{-1}$) was shown by the linear regression from 15 to 30 °C as follows:

$$\delta^{18}\text{O}_{\text{Otolith,PDB}} - \delta^{18}\text{O}_{\text{seawater,SMOW}} = -0.153 \times T(^{\circ}\text{C}) + 1.418 (r^2 = 0.95) \quad (2)$$

The relationship between oxygen isotopic composition and temperature is also presented as follows:

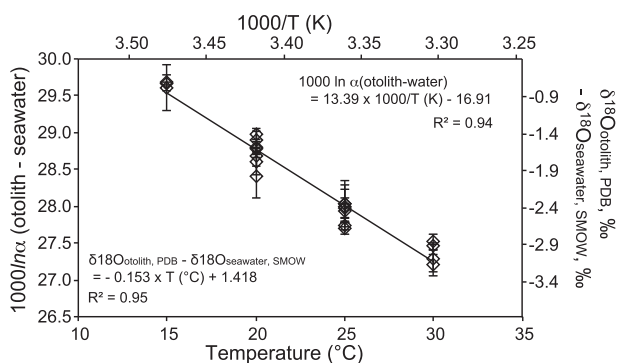


Fig. 3. Correlation of the fractionation between otolith of Japanese eel and seawater with water temperature. Temperature and fractionation factor are also presented in $1000/T$ and difference of delta values ($\delta^{18}\text{O}_{\text{Otolith,PDB}} - \delta^{18}\text{O}_{\text{seawater,SMOW}}$) at upper horizontal and right vertical axes, respectively. Each data point shows the average for individual otolith.

Table 3

$\delta^{18}\text{O}$ values of otolith core region and ambient water temperature on wild-caught glass eels estimated by the otolith $\delta^{18}\text{O}$ values.

Collection sites of glass eel	s	Otolith $\delta^{18}\text{O}$ (‰, PDB)	Estimated water temperature (°C)
Tone River	1	-2.55 ± 0.19	26.4
	2	-2.69 ± 0.19	27.3
	3	-2.42 ± 0.19	25.5
	4	-2.46 ± 0.11	25.8
	Mean	-2.53 ± 0.12	26.3 ± 0.8
Hamana Lake	1	-2.58 ± 0.41	26.6
	2	-2.57 ± 0.25	26.5
	3	-2.69 ± 0.32	27.3
	4	-2.53 ± 0.13	26.3
	Mean	-2.59 ± 0.07	26.7 ± 0.4

Mean (\pm SD) of eight temperatures was $26.5 (\pm 0.6)$ °C. Error of each analysis was assigned from the reproducibility of UWC-3 (2SD). Estimation of water temperature by otolith $\delta^{18}\text{O}$ is by the equation: $\delta^{18}\text{O}_{\text{Otolith,PDB}} - \delta^{18}\text{O}_{\text{seawater,SMOW}} (=0.06\text{‰}) = -0.153 \times T(^{\circ}\text{C}) + 1.418$.

$$1000 \ln \alpha (\text{otolith} - \text{water}) = 13.39 \times 1000/T(\text{K}) - 16.91 (r^2 = 0.94) \quad (3)$$

where $\alpha (\text{otolith-water}) = (\delta^{18}\text{O}_{\text{Otolith,PDB}} + 1000) / (\delta^{18}\text{O}_{\text{seawater,PDB}} + 1000)$.

The ranges and means of $\delta^{18}\text{O}_{\text{Otolith,PDB}}$ of the otolith core region of 8 of the glass eels collected from Hamana Lake and the Tone River were -2.42 to -2.69 and -2.53 ± 0.12 (‰ \pm SD), and -2.53 to -2.69 and -2.59 ± 0.07 , respectively (Table 3). There was no significant difference in the $\delta^{18}\text{O}$ values between the glass eels from the two sampling sites (Mann-Whitney U -test, $p < 0.05$). Oxygen isotopic composition of seawater during the core formation was estimated from data obtained from as near as possible to the spawning/hatching site (122.99 °E, 16.52 °N) in June 1974, and to be 0.06‰ (averaged value of possible depth, -0.03‰ at 103 m, 0.05‰ at 168 m, 0.16‰ at 226 m, and 0.06‰ at 324 m) (Östlund et al., 1987). By assuming this seawater oxygen isotopic composition, the $\delta^{18}\text{O}$ values of the otolith core regions could be converted to 26.3 – 27.3 °C for glass eels from the Hamana Lake and 25.5 – 27.3 °C for those from the Tone River using equation (Eq. (3)) that expressed the relationship between otolith $\delta^{18}\text{O}$ values without correction of possible effects of isotope composition in rearing water and ambient water temperature. The mean (\pm SD) of the estimated temperature of the eight glass eels was 26.5 ± 0.6 °C, suggesting that each glass eel had experienced a water temperature environment of about 26 – 27 °C during the incubation period after primordium formation. When otolith core $\delta^{18}\text{O}$ values were simply converted to temperature without correction of the $\delta^{18}\text{O}_{\text{seawater}}$ using Eq. (1), estimated temperature showed similar value of 25.9 ± 0.7 °C. The water depths corresponding to those estimated temperatures were at ~ 150 m in the water column, which almost corresponds to the upper-most part of the thermocline and chlorophyll maximum in the vertical profile of water temperature in the spawning area of the Japanese eel (Fig. 4; Tsukamoto et al., 2011).

Inter- and intra-otolith variations in rate of otolith growth outside of the ALC mark, corresponding to the precipitation rate of aragonite during the 30-day rearing period, were found in glass eels reared at a constant water temperature (Fig. 5). The ranges of otolith radial growth

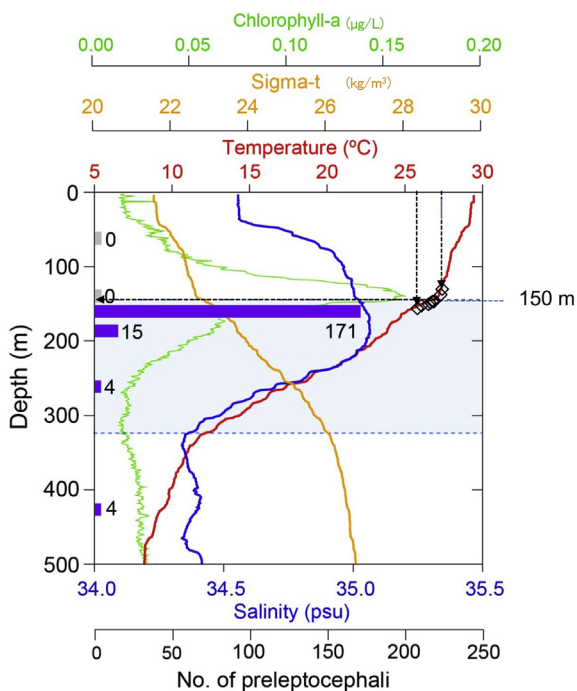


Fig. 4. Depth distribution of Japanese eel preleptocephali and environmental parameters plotted by depth from the ocean surface in the spawning area, and the estimated temperature of egg distribution (modified from Tsukamoto et al., 2011 Fig. 6). The number of preleptocephali that were collected at each depth stratum is shown by blue bars. The thermocline is shown by pale blue area between dotted lines and is the area of most rapid change in water temperature (red line) with depth. The large increase in chlorophyll concentration (green line) at around 150 m also occurred at the top of the thermocline. Sigma-t (orange line) is a measure of water density that is calculated from both salinity (blue line) and temperature. The estimated temperature of egg distribution (25.5–27.3 °C, diamonds) corresponds to the depth about 150 m in the uppermost portion of the thermocline. (For interpretation of the references to colour in this figure legend, the reader is referred to the web version of this article.)

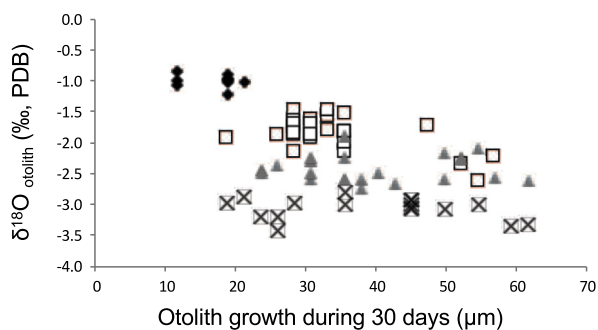


Fig. 5. The relationship between otolith $\delta^{18}\text{O}$ and otolith growth rate of Japanese eel glass eels reared at temperatures of 15 (◆), 20 (□), 25 (▲) and 30 (×) °C.

in 30 days were 10–20 μm at 15 °C and 20–60 μm at and above 20 °C (Fig. 5). The average growth rate over the 30 days incubation period ranged from $17 \pm 4 \mu\text{m}$ at 15 °C to $39 \pm 13 \mu\text{m}$ at 30 °C (Table 2). The otolith growth rate

at 15 °C was markedly lower than those in the other higher temperature treatments (Fig. 5). The $\delta^{18}\text{O}$ values of the otolith edge outside the ALC mark were fairly homogeneous and were almost all included within the 95% confidence interval for each water temperature treatment (Fig. 5). Growth or precipitation rate dependent oxygen isotopic fractionations are reported for inorganically precipitated calcite at both a bulk scale (Dietzel et al., 2009) and a micrometer scale (Gabitov et al., 2012), however this was not the case for eel otoliths. This suggests that otolith radial growth rate may have little effect on the fractionation of $\delta^{18}\text{O}$ values in otolith aragonite, and individual $\delta^{18}\text{O}$ data obtained by ion microprobe reflects representative value of the growth timing.

4. DISCUSSION

The present study is the first to examine eel otoliths using the secondary ion mass spectrometry (SIMS) microanalysis technique to estimate the temperature environment where the eggs of the Japanese eel develop and hatch. Equation (2) shows that the temperature dependence of otolith $\delta^{18}\text{O}$ is inversely related ($-0.153\text{‰ } ^\circ\text{C}^{-1}$) in the Japanese eel. Similar inverse relationships between otolith $\delta^{18}\text{O}$ values and ambient water temperature have been reported in several fish species (Kalish, 1991a,b; Radtke et al., 1996; Thorrold et al., 1997; Høie et al., 2004; Kitagawa et al., 2013; Table 4). The slope and intercept of the temperature dependence curve (Fig. 6, Table 4) of oxygen isotope fractionation ($1000 \ln \alpha(\text{otolith-water})$) of glass eel otoliths in the present study seem to be slightly different from the values given by previous studies for fish species (Kalish, 1991a,b; Patterson et al., 1993; Radtke et al., 1996; Thorrold et al., 1997; Høie et al., 2004; Kitagawa et al., 2013). The slope of the temperature dependence of glass eel otoliths in the present study (13.39) is smaller (shallower slope) than the values given by previous studies for fish species such as Atlantic cod (*Gadus morhua*) (18.70, Radtke et al. 1996, 1998, 16.75, Høie et al., 2004), Atlantic croaker (*Micropogonias undulatus*) (18.56, Thorrold et al., 1997) and Pacific bluefin tuna larvae (*Thunnus orientalis*) (24.28, Kitagawa et al., 2013) as well as for inorganic aragonite (17.88, Kim et al., 2007) and inorganic calcite (18.03, Kim and O'Neil, 1997) (Table 4, Fig. 6). The lower survival rate of the glass eels reared at 30 °C (74% vs. 100% survival at other temperatures) and the fewer increments deposited in the otoliths of the glass eels reared at 15 °C during the 30-day rearing period compared to fish at 25–30 °C that formed complete daily increments (Fukuda et al., 2009) indicated those temperatures affected the physiology of glass eels. Those higher and lower temperatures may cause some physiological stress that might also potentially influence otolith $\delta^{18}\text{O}$ values and consequently the slope of the regression. However, because of possible systematic differences in the matrix effects during SIMS analysis for aragonite samples vs. calcite standards, it is difficult to determine whether the difference of the curves is the real or an analytical artefact. It should be noted that the temperature calibration of the otolith core data was obtained from the reared eel otoliths for which matrix matches otoliths from wild eels, thus any differences in

Table 4

Temperature dependence of oxygen isotope fractionation ($1000 \ln \alpha$ (otolith-seawater)) in this study and the literature.

Reference	Species	Equations	Temperature range (°C)
This study	<i>Anguilla japonica</i>	$1000 \ln \alpha = 13.39 \times (1000/T) - 16.91$	15–30
Kim et al. (2007)	Inorganic aragonite	$1000 \ln \alpha = 17.88 \times (1000/T) - 31.14$	0–40
Patterson et al. (1993)	Several freshwater fish species	$1000 \ln \alpha = 18.56 \times (1000/T) - 33.49$	0–40
Thorrold et al. (1997)	<i>Micropogonias undulatus</i>	$1000 \ln \alpha = 18.56 \times (1000/T) - 32.54$	3.2–30.3
Radtke et al. (1996)	<i>Gadus morhua</i>	$1000 \ln \alpha = 18.70 \times (1000/T) - 33.13$	18.2–25
Høie et al. (2004)	<i>Gadus morhua</i>	$1000 \ln \alpha = 16.75 \times (1000/T) - 27.09$	9.0–16.0
Kitagawa et al. (2013)	<i>Thunnus orientalis</i>	$1000 \ln \alpha = 24.28 \times (1000/T) - 52.83$	23.0–27.0
Kim and O'Neil (1997)	Inorganic calcite	$1000 \ln \alpha = 18.03 \times (1000/T) - 32.42$	10–40

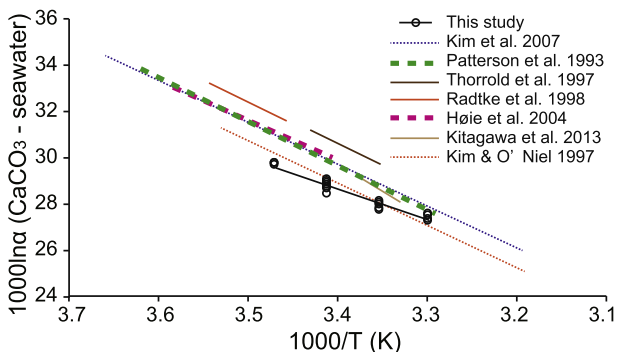


Fig. 6. Comparison of the fractionation factor (otolith-seawater) obtained in the present study with that of otoliths as well as inorganic calcite and aragonite published in the literature. Fractionation factor and temperature are presented as $1000 \ln \alpha$ on vertical axis and $1000/T$ (K) on horizontal axis, respectively.

matrix effect will be canceled out and the accuracy of calibrated hatching temperatures should not be affected.

The otolith thermometry of the present study targeted the otolith core region of glass eels and strongly suggested that the eggs of the Japanese eel occurred at a depth layer of about 150 m in the water column in the spawning area (Table 3, Fig. 4). The prediction of this depth layer based on otolith $\delta^{18}\text{O}$ values (data first obtained in 2008; Shirai et al., 2010) directly contributed to the discovery and first recovery of Japanese eel eggs around the southern part of the West Mariana Ridge by Tsukamoto et al. (2011), before the present study was published. These data led net sampling for eggs to be focused on more shallow layers (upper 200 m) in water over 3000 m deep, which markedly decreased the amount of time and effort for each net towing, thus increasing the efficiency of fishing and the chances of finding eggs. Fertilized eggs and recently hatched preleptocephali also have been collected from the depth layer of 150–170 m at the upper-most part of the thermocline and around the chlorophyll maximum in the water column (Fig. 4; Tsukamoto et al., 2011; Aoyama et al., 2014), which is close to the depth of the egg occurrence estimated by otolith $\delta^{18}\text{O}$ values. On the other hand, eels may spawn in the depth layer of 180–320 m as suggested by Kurogi et al. (2011) who captured post-spawning female Japanese eels in their spawning area. The expected spawning depth of 180–320 m (corresponding temperatures are 24–13 °C) will produce otolith oxygen isotopic composition of -2.2 to -0.5‰ using Eq. (1), which is significantly lower than the

observed values of otolith cores. The otolith isotopic signature indicates that egg development in the latter half of the incubation period, hatching, and early development may all occur at a depth layer of ~ 150 m. Pelagic eel eggs may immediately float up after spawning and become retained under the thermocline until the hatching. This behavior is supported by both field egg/preleptocephali collections and otolith isotopic signatures. The Japanese eel eggs and newly hatched larvae possibly become neutrally buoyant compared to the seawater at about 26–27 °C, which corresponds to the upper layer of the thermocline. This is consistent with the experimental result by Tsukamoto et al. (2009b) that the specific gravity of artificially produced eggs and preleptocephali of Japanese eel were around those of the seawater at 22–26 °C, which roughly corresponded to the water temperature at depths of 200–100 m in the North Equatorial Current (15°N, 140°E). It should be noted that these values of temperature and depth were estimated from the on-site environmental parameters from which the Japanese eel eggs and preleptocephali were actually collected. No significant difference in $\delta^{18}\text{O}_{\text{otoliths}}$ between two populations from different year class (Tone river in 1998 for Sample-A and Hamana Lake in 2006 for Sample-B) may indicate that the spawning eels actively chose a favorable condition for spawning (i.e. temperature and salinity), irrespective of variability in annual change of local environmental settings. Since the adequate spawning location varies inter-annually depending on the environmental settings of spawning timing (Aoyama et al., 2014), similar $\delta^{18}\text{O}_{\text{otolith}}$ values between two populations may indicate that temperature and salinity for hatching is important factor to determine a spawning location for Japanese eel.

The narrow range of temperatures estimated by the $\delta^{18}\text{O}$ values of the eight glass eel otolith core regions in this study indicates that the eel eggs stayed in a limited range of temperatures during the incubation period at least after primordium formation. The primordium of the otoliths of Japanese eels is formed at about 15–18 h after fertilization during an incubation period of 27–32 h at 25 °C in the laboratory (Ahn et al., 2012). The analysis spots for SIMS analysis were randomly distributed on the surface of the otolith core region, and the constant $\delta^{18}\text{O}$ values of the otolith core region indicate that the oxygen isotope composition was constant within the otolith core region. The eggs may have accumulated and been retained around the thermocline until they hatched. The thermocline, also usually a pycnocline or density gradient, may function like a ceiling for trapping eggs that float up from the possibly deeper

spawning depth layer. Okamura et al. (2007) suggested that the optimal temperature for eggs and pre-feeding larvae of Japanese eels is approximately 25–28 °C. Kurokawa et al. (2008) reported the most suitable temperature for rearing without deformities to be 24–26 °C in Japanese eels. These reports agree with the present findings on the temperatures experienced during the egg stage. Early larval development around the thermocline and chlorophyll maximum would also likely be advantageous for the feeding of eel larvae, which feed on marine snow (Otake et al., 1993; Miller et al., 2013) because marine snow is produced in the upper few hundred meters including within the chlorophyll maximum (Ichikawa, 1982; Hebel and Karl, 2001) it may often accumulate around the pycnocline (MacIntyre et al., 1995).

The present study applied SIMS for otolith oxygen isotope micro-analysis with lateral spatial resolution of 8 µm and provided $\delta^{18}\text{O}$ values of the otolith core region of glass eels to estimate the water temperature where Japanese eel eggs develop. The estimated depth layer of ~150 m where eggs may be distributed was predicted based on the rearing experiments and confirmed by field sampling data of eel eggs and larvae. The small beam size and the ability to analyze areas as close as several microns, together with improved precision, allow otolith isotope profiles to be obtained with daily resolution as Hanson et al. (2010) suggested. The present study shows that stable isotope micro-analysis provides important new information for ecology on the early life history of eels, as well as for unknown migration ecology of fishes. Future studies using this technique may shed light on the spawning depths of other anguillid eels and on the depths used by their leptocephali later during their early life history.

ACKNOWLEDGEMENTS

The authors thank Dr. Akira Shinoda of the Tokyo Medical University for providing the glass eels collected from Tone River, and Dr. Michael J. Miller of the Nihon University, for improving the manuscript. This work was supported in part by the Ministry of Education, Culture, Sports, Science and Technology (MEXT) Grants in Aid No. 21380122 and 24380105 (P.I. Tsuguo Otake), No. JP16KT0028 (P.I. Kotaro Shirai) and No. 21228005 (P.I. Katsumi Tsukamoto) to Atmosphere and Ocean Research Institute, The University of Tokyo. The WiscSIMS Laboratory is funded by the US-NSF (EAR-0319230, 1053466, 1355590, 1658823). Kotaro Shirai and Tsuguo Otake contributed equally to this work.

APPENDIX A. SUPPLEMENTARY MATERIAL

Supplementary data associated with this article can be found, in the online version, at <https://doi.org/10.1016/j.gca.2018.03.006>.

REFERENCES

Ahn H., Yamada Y., Okamura A., Horie N., Mikawa N., Tanaka S. and Tsukamoto K. (2012) Effect of water temperature on

- embryonic development and hatching time of the Japanese eel *Anguilla japonica*. *Aquaculture* **330**, 100–105.
- Aoyama J., Watanabe S., Miller M. J., Mochioka N., Otake T., Yoshinaga T. and Tsukamoto K. (2014) Spawning sites of the Japanese eel in relation to oceanographic structure and the West Mariana Ridge. *PLoS One* **9**, e88759.
- Begg G. A. and Weidman C. R. (2001) Stable d^{13}C and d^{18}O isotopes in otoliths of haddock *Melanogrammus aeglefinus* from the northwest Atlantic Ocean. *Mar. Ecol. Prog. Ser.* **216**, 223–233.
- Campana S. E. (1999) Chemistry and composition of fish otoliths: pathways, mechanisms and applications. *Mar. Ecol. Prog. Ser.* **188**, 263–297.
- Casselman J. M. (2003) Dynamics of resources of the American eel, *Anguilla rostrata*: declining abundance in the 1990s. In *Eel Biology* (eds. K. Aida, K. Tsukamoto and K. Yamauchi). Springer, Tokyo, pp. 255–274.
- Chow S., Kurogi H., Mochioka N., Kaji S., Okazaki M. and Tsukamoto K. (2009) Discovery of mature freshwater eels in the open ocean. *Fish. Sci.* **75**, 257–259.
- Coplen T. B., Kendall C. and Hopple J. (1983) Comparison of stable isotope reference samples. *Nature* **302**(5905), 236.
- Dekker W. (2003) Status of the European eel stock and fisheries. In *Eel Biology* (eds. K. Aida, K. Tsukamoto and K. Yamauchi). Springer, Tokyo, pp. 237–254.
- Dietzel M., Tang J., Leis A. and Köhler S. J. (2009) Oxygen isotopic fractionation during inorganic calcite precipitation—Effects of temperature, precipitation rate and pH. *Chem. Geol.* **268**, 107–115.
- Epstein S. and Mayeda T. (1953) Variation of O^{18} content of waters from natural sources. *Geochim. Cosmochim. Acta* **4**, 213–224.
- Feunteun E. (2002) Management and restoration of European eel population (*Anguilla anguilla*): an impossible bargain. *Ecol. Eng.* **18**, 575–591.
- Friedland K. D., Miller M. J. and Knights B. (2007) Oceanic changes in the Sargasso Sea and declines in recruitment of the European eel *ICES J. Mar. Sci.: Journal du Conseil*. **64**, 519–530.
- Fukuda N., Kuroki M., Shinoda A., Yamada Y., Okamura A., Aoyama J. and Tsukamoto K. (2009) Influence of water temperature and feeding regime on otolith growth in *Anguilla japonica* glass eels and elvers: does otolith growth cease at low temperatures? *J. Fish Biol.* **74**, 1915–1933.
- Gabitov R. I., Watson E. B. and Sadekov A. (2012) Oxygen isotope fractionation between calcite and fluid as a function of growth rate and temperature: An in situ study. *Chem. Geol.* **306**, 92–102.
- Gao Y. W. and Beamish R. J. (1999) Isotopic composition of otoliths as a chemical tracer in population identification of sockeye salmon (*Oncorhynchus nerka*). *Can. J. Fish. Aquat. Sci.* **56**, 2062–2068.
- Gao Y. W. and Beamish R. J. (2003) Stable isotope variations in otoliths of Pacific halibut (*Hippoglossus stenolepis*) and indications of the possible 1990 regime shift. *Fish. Res.* **60**, 393–404.
- Gao Y. W., Joner S. H. and Bargmann G. G. (2001a) Stable isotopic composition of otoliths in identification of spawning stocks of Pacific herring (*Clupea pallasii*) in Puget Sound. *Can. J. Fish. Aquat. Sci.* **58**, 2113–2120.
- Gao Y. W., Schwarcz H. P., Brand U. and Moksness E. (2001b) Seasonal stable isotope records of otoliths from ocean-pen reared and wild cod, *Gadus morhua*. *Environ. Biol. Fish.* **61**, 445–453.
- Geffen A. J. (2012) Otolith oxygen and carbon stable isotopes in wild and laboratory-reared plaice (*Pleuronectes platessa*). *Environ Biol Fish.* **95**, 419–430.

- Hanson N. N., Wurster C. M. and Todd C. D. (2010) Comparison of secondary isotope ratio mass spectrometry and micromilling/continuous flow isotope ratio mass spectrometry techniques used to acquire intra-otolith $\delta^{18}\text{O}$ values of wild Atlantic salmon (*Salmo salar*). *Rapid Commun. Mass Spectrom.* **24**, 2491–2498.
- Hebel D. V. and Karl D. M. (2001) Seasonal, interannual and decadal variations in particulate matter concentrations and composition in the subtropical North Pacific Ocean. *Deep-Sea Res. II* **48**, 1669–1695.
- Hogan J. D., Kozdon R., Blum M. J., Gilliam J. F., Valley J. W. and McIntyre P. B. (2017) Reconstructing larval growth and habitat use in an amphidromous goby using otolith increments and microchemistry. *J. Fish Biol.* **90**, 1338–1355.
- Høie H., Otterlei E. and Folkvord A. (2004) Temperature-dependent fractionation of stable oxygen isotopes in otoliths of juvenile cod (*Gadus morhua* L.). *ICES J. Mar. Sci.: Journal du Conseil.* **61**, 243–251.
- ICES. (2010) Report of the joint EIFAC/ICES Working Group on eels (WGEEEL), September 2010. Rep No ICES CM 2010/ACOM.18, Hamburg Germany. pp. 9–14.
- Ichikawa T. (1982) Particulate organic carbon and nitrogen in the adjacent seas of the Pacific Ocean. *Mar. Biol.* **68**, 49–60.
- Jacoby D. M. P., Casselman J. M., Crook V., DeLucia M. B., Ahn H., Kaifu K., Kurwie T., Sasal P., Silfvergrip A. M. C., Smith K. G., Uchidal K., Walkerm A. M. and Gollock M. J. (2015) Synergistic patterns of threat and the challenges facing global anguillid eel conservation. *Glob. Ecol. Conserv.* **4**, 321–333.
- Kalish J. M. (1991a) Oxygen and carbon stable isotopes in the otoliths of wild and laboratory-reared Australian salmon (*Arripis trutta*). *Mar. Biol.* **110**, 37–47.
- Kalish J. M. (1991b) ^{13}C and ^{18}O isotopic disequilibria in fish otoliths: metabolic and kinetic effects. *Mar. Ecol. Prog. Ser.* **75**, 191–203.
- Kim S. T. and O'Neil J. R. (1997) Equilibrium and nonequilibrium oxygen isotope effects in synthetic carbonates. *Geochim. Cosmochim. Acta* **61**, 3461–3475.
- Kim S. T., O'Neil J. R., Hillaire-Marcel C. and Mucci A. (2007) Oxygen isotope fractionation between synthetic aragonite and water: influence of temperature and Mg^{2+} concentration. *Geochim. Cosmochim. Acta* **71**, 4704–4715.
- Kita N. T., Ushikubo T., Fu B. and Valley J. W. (2009) High precision SIMS oxygen isotope analysis and the effect of sample topography. *Chem. Geol.* **264**, 43–57.
- Kitagawa T., Ishimura T., Uozato R., Shirai K., Amano Y., Shinoda A., Otake T., Tsunogai U. and Kimura S. (2013) Otolith $\delta^{18}\text{O}$ of Pacific bluefin tuna *Thunnus orientalis* as an indicator of ambient water temperature. *Mar. Ecol. Prog. Ser.* **481**, 199–209.
- Knights B. (2003) A review of the possible impacts of long-term oceanic and climate changes and fishing mortality on recruitment of anguillid eels of the Northern Hemisphere. *Sci. Total Environ.* **310**, 237–244.
- Kozdon R., Ushikubo T., Kita N. T., Spicuzza M. and Valley J. W. (2009) Intratest oxygen isotope variability in the planktonic foraminifer *N. pachyderma*: Real vs. apparent vital effects by ion microprobe. *Chem. Geo.* **258**, 327–337.
- Kurogi H., Okazaki M., Mochioka N., Jinbo T., Hashimoto H., Takahashi M., Tawa A., Aoyama J., Shinoda A., Tsukamoto K., Tanaka H., Gen K., Kazeto Y. and Chow S. (2011) First capture of post-spawning female of the Japanese eel *Anguilla japonica* at the southern West Mariana Ridge. *Fish. Sci.* **77**, 199–205.
- Kurokawa T., Okamoto T., Gen K., Uji S., Murashita K., Unuma T., Nomura K., Matsubara H., Kim S. K., Ohta H. and Tanaka H. (2008) Influence of water temperature on morphological deformities in cultured larvae of Japanese eel, *Anguilla japonica*, at completion of yolk resorption. *J. World Aquacult. Soc.* **39**, 726–735.
- Kuroki M., Righton D. and Walker A. M. (2014) The importance of Anguillids: a cultural and historical perspective introducing papers from the World Fisheries Congress. *Ecol. Freshw. Fish* **23**, 2–6.
- Kuroki M., Okamura A., Takeuchi A. and Tsukamoto K. (2016) Effect of water current on the body size and occurrence of deformities in reared Japanese eel leptocephali and glass eels. *Fish. Sci.* **82**, 941–951.
- Lecomte-Finiger R. (1994) The early-life of the European eel. *Nature* **370**, 424.
- Limburg K. E., Hayden T. A., Pine, III, W. E., Yard M. D., Kozdon R. and Valley J. W. (2013) Of Travertine and Time: Otolith Chemistry and Microstructure Detect Provenance and Demography of Endangered Humpback Chub in Grand Canyon, USA. *PLoS one.* **8**, e84235.
- Linzmeier B. J., Kozdon R., Peters S. E. and Valley J. W. (2016) Oxygen isotope variability within nautilus shell growth bands. *PLoS One.* **11**, e0153890.
- MacIntyre S., Alldredge A. L. and Gotschalk C. C. (1995) Accumulation of marine snow at density discontinuities in the water column. *Limnol. Oceanogr.* **40**, 449–468.
- Matta M. E., Orland I. J., Ushikubo T., Helser T. E., Black B. A. and Valley J. W. (2013) Otolith oxygen isotopes measured by high-precision secondary ion mass spectrometry reflect life history of a yellowfin sole (*Limanda aspera*). *Rapid Commun. Mass Spectrom.* **27**, 691–699.
- McConnaughey T. (1989) ^{13}C and ^{18}O isotopic disequilibrium in biological carbonates: I. Patterns. *Geochim. Cosmochim. Acta* **53**, 151–162.
- Miller M. J., Kimura S., Friedland K. D., Knights B., Kim H., Jellyman D. J. and Tsukamoto K. (2009) Review of ocean-atmospheric factors in the Atlantic and Pacific oceans influencing spawning and recruitment of anguillid eels. In *Challenges for Diadromous Fishes in a Dynamic Global Environment* (eds. A. J. Haro, K. L. Smith, R. A. Rulifson, C. M. Moffitt, R. J. Klauda, M. J. Dadswell, R. A. Cunjak, J. E. Cooper, K. L. Beal and T. S. Avery). Am Fish Soc Symp, Bethesda Maryland, pp. 231–249.
- Miller M. J., Chikaraishi Y., Ogawa N. O., Yamada Y., Tsukamoto K. and Ohkouchi N. (2013) A low trophic position of Japanese eel larvae indicates feeding on marine snow. *Biol. Lett.* **9**, 20120826.
- Morat F., Letourneur Y., Dierking J., Pécheyran C., Bareille G., Blamart D. and Harmelin-Vivien M. (2014) The great melting pot. Common sole population connectivity assessed by otolith and water fingerprints. *PLoS One* **9**, e86585.
- Okamoto T., Kurokawa T., Gen K., Murashita K., Nomura K., Kim S. K., Matsubara H., Ohta H. and Tanaka H. (2009) Influence of salinity on morphological deformities in cultured larvae of Japanese eel, *Anguilla japonica*, at completion of yolk resorption. *Aquaculture* **293**, 113–118.
- Okamura A., Yamada Y., Horie N., Utoh T., Mikawa N., Tanaka S. and Tsukamoto K. (2007) Effects of water temperature on early development of Japanese eel *Anguilla japonica*. *Fish. Sci.* **73**, 1241–1248.
- Orland I. J., Kozdon R., Linzmeier B., Wycech J., Sliwinski M., Kitajima K., Kita N. T. and Valley J. W. Enhancing the accuracy of carbonate $\delta^{18}\text{O}$ and $\delta^{13}\text{C}$ measurement by SIMS. AGU Fall meeting, Dec. 14–18, 2015, San Francisco. Abstr. #: PP52B-03.
- Östlund G. H., Craig, H. C., Broecker W. S., Spencer D. W. and GEOSECS (1987) Shorebased measurements during the GEOSECS Pacific expedition. PANGAEA, 10.1594/PANGAEA.743238.

- Otake T., Nogami K. and Maruyama K. (1993) Dissolved and particulate organic-matter as possible food sources for eel leptocephali. *Mar. Ecol. Prog. Ser.* **92**, 27–34.
- Patterson W. P., Smith G. R. and Lohmann K. C. (1993) Continental paleothermometry and seasonality using the isotopic composition of aragonitic otoliths of freshwater fishes. *Climate Change Continental Isotopic Records, Am. Geophys. Union Monogr.*, 191–202.
- Radtke R. L., Lenz P., Showers W. and Moksness E. (1996) Environmental information stored in otoliths: insights from stable isotopes. *Mar. Biol.* **127**, 161–170.
- Sano Y., Shirai K., Takahata N., Amakawa H. and Otake T. (2008) Ion microprobe Sr isotope analysis of carbonates with about 5 μ m spatial resolution: An example from an ayu otolith. *Appl. Geochem.* **23**, 2406–2413.
- Schabetsberger R., Miller M. J., Olmo G. D., Kaiser R., Økland F., Watanabe S., Aarestrup K. and Tsukamoto K. (2016) Hydrographic features of anguillid spawning areas: potential signposts for migrating eels. *Mar. Ecol. Prog. Ser.* **554**, 141–155.
- Shephard S., Trueman C., Rickaby R. and Rogan E. (2007) Juvenile life history of NE Atlantic orange roughy from otolith stable isotopes. *Deep-Sea Res I.* **54**, 1221–1230.
- Shirai K., Otake T., Kuroki M., Ushikubo T., Kita N. T., Amano Y. and Tsukamoto K. (2010) Eel larvae may hatch in the surface layer near the West Mariana Ridge: ion microprobe delta O-18 analysis with 7 μ m spatial resolution in glass eel otoliths. *Geochim. Cosmochim. Acta* **74**, A955.
- Śliwiński M. G., Kitajima K., Spicuzza M. J., Orland I. J., Ishida A., Fournelle J. H. and Valley J. W. (2017) SIMS bias on isotope ratios in Ca-Mg-Fe carbonates (Part III): $\delta^{18}\text{O}$ and $\delta^{13}\text{C}$ matrix effects along the magnesite-siderite solid-solution series. *Geostand. Geoanal. Res.* **42**, 49–76.
- Tanaka H. (2011) Studies on artificial fry production of Japanese eel. *Nippon Suisan Gakkaishi* **77**, 345–351 (in Japanese with English abstract).
- Thorrold S. R., Campana S. E., Jones C. M. and Swart P. K. (1997) Factors determining $\delta^{13}\text{C}$ and $\delta^{18}\text{O}$ fractionation in aragonitic otoliths of marine fish. *Geochim. Cosmochim. Acta* **61**, 2909–2919.
- Tsukamoto K. (2006) Spawning of eels near a seamount. *Nature* **439**, 929.
- Tsukamoto K., Aoyama J. and Miller M. J. (2009a) Present status of the Japanese eel: resources and recent research. In *Eels at the edge: Am Fish Soc Symp* **58**, pp. 21–35.
- Tsukamoto K., Chow S., Otake T., Kurogi H., Mochioka N., Miller M. J., Aoyama J., Kimura S., Watanabe S., Yoshinaga T., Shinoda A., Kuroki M., Oya M., Watanabe T., Hata K., Ijiri S., Kazeto Y., Nomura K. and Tanaka H. (2011) Oceanic spawning ecology of freshwater eels in the western North Pacific. *Nat. Commun.* **2**, 179.
- Tsukamoto K., Yamada Y., Okamura A., Kaneko T., Tanaka H., Miller M. J., Horia N., Mikawa N., Utoh T. and Tanaka S. (2009b) Positive buoyancy in eel leptocephali: an adaptation for life in the ocean surface layer. *Mar. Biol.* **156**, 835–846.
- Valley J. W. and Kita N. T. (2009) In situ oxygen isotope geochemistry by ion microprobe. *MAC Short Course: Secondary Ion Mass Spectrometry Earth Sci.* **41**, 19–63.
- Walther B. D. and Thorrold S. R. (2009) Inter-annual variability in isotope and elemental ratios recorded in otoliths of an anadromous fish. *J. Geochem. Explor.* **102**, 181–186.
- Wanamaker A. D., Kreutz K. J., Borns H. W., Introne D. S., Feindel S., Funder S., Rawson P. D. and Barber B. J. (2007) Experimental determination of salinity, temperature, growth, and metabolic effects on shell isotope chemistry of *Mytilus edulis* collected from Maine and Greenland. *Paleoceanography* **22**. <https://doi.org/10.1029/2006PA001352>.
- Weber P. K., Bacon C. R., Hutcheon I. D., Ingram B. L. and Wooden J. L. (2005) Ion microprobe measurement of strontium isotopes in calcium carbonate with application to salmon otoliths. *Geochim. Cosmochim. Acta* **69**, 1225–1239.
- Weidel B. C., Ushikubo T., Carpenter S. R., Kita N. T., Cole J. J., Kitchell J. F., Pace M. L. and Valley J. W. (2007) Diary of a bluegill (*Lepomis macrochirus*): daily $\delta^{13}\text{C}$ and $\delta^{18}\text{O}$ records in otoliths by ion microprobe. *Can. J. Fish. Aquat. Sci.* **64**, 1641–1645.

Associate editor: Thomas M. Marchitto